Design, fabrication, and preclinical testing of a miniaturized, multispectral, chip-on-tip, imaging probe for intraluminal fluorescence imaging of the gastrointestinal tract

Authors: Bridget Slomka, Suzann Duan, Ricky Sontz, Juanita L. Merchant, Travis W. Sawyer

Abstract

As gastrointestinal cancers continue to cause a disproportionately large percentage of annual cancer deaths in the US, advancements in miniature imaging technology combined with a need for precise and thorough tumor detection in gastrointestinal cancer screenings fuel the demand for new, small-scale, and low-cost methods of localization and margin detection with improved accuracy. A miniaturized, chip-on-tip, multispectral, fluorescence imaging probe designed to port through a gastroscope working channel has been developed for detection of cancerous lesions in the gut lumen in point of care gastrointestinal endoscopy. Preclinical testing has confirmed fluorescence sensitivity and supports that this miniature probe can locate structures of interest via detection of fluorescence emission from exogenous contrast agents. This work demonstrates the design and preliminary performance evaluation of a miniaturized, single-use, chip-on-tip fluorescence imaging system devised for deployment via the accessory channel of a standard gastroscope.

Introduction

The clinical use of endoscopic imaging devices remains critical to the discovery of malignancies manifesting in internal luminal organs such as those of the gastrointestinal (GI) tract. As endoscopes continue to improve in resolution, sensitivity, and operability within tight spaces, so too has clinicians' ability to visualize subtle morphological and functional changes indicative of pathogenesis in a variety of tissues, diseases, and procedures. For example, endoscopic devices are now commonly used in combination with surgical tools for performing complex laparoscopic operations to improve clinical outcomes in oncologic surgery.[1] Fluorescence-guided surgery (FGS), in particular, has shown promise by significantly improving the visual contrast between normal and cancerous tissues, therefore facilitating the complete resection of tumors which may reduce the likelihood of their recurrence.[2,3] As such, FGS has the potential to serve as a means for effective localization, visual inspection, and complete surgical resection of tumors within the GI tract. Fluorescence imaging is one method that has shown success for delineating healthy tissues from those that are cancerous. By tagging specific biomarkers in cancer tissue with exogenous fluorescent moieties, contrast can be induced between highly fluorescent cancerous tissue and minimally fluorescent normal tissue. Thus, endoscopic fluorescence imaging may serve to improve the sensitivity of screenings and support the complete resection of tumors during FGS. Using tumor-specific antibodies labeled with fluorescent dyes, researchers have demonstrated effective tumor localization in both human and animal studies involving GI cancers.[2–4] In these works, laparoscopic fluorescence imaging was employed for the visualization of molecular probes that bind to carcinoembryonic antigen (CEA), an embryonic protein that is frequently expressed in large quantities by adults with some forms of cancer.[3] Administered intravenously before surgery, these fluorophore-labeled, anti-CEA monoclonal antibodies improved clinicians' ability to detect and completely resect colorectal tumors and are now being evaluated in further clinical trials that

aim to demonstrate their efficacy for improving the treatment of multiple GI cancers.[5] Similar research with octreotide conjugates for targeted delivery of fluorescent tags to GI cancers that do not express CEA is also underway, highlighting the advancement of fluorescent probes in the detection of cancerous lesions.[6]

Endoscopy of the GI tract is generally performed with broadband illumination. However, current implementations of white light endoscopy (WLE), which have been proven less sensitive than other methods of imaging, like narrowband and chromoendoscopy, may not be sensitive enough to resolve subtle indications like those of precancerous lesions.[7,8] The sensitivity of WLE is limited by the operator's ability to detect subtle changes in color, texture, and form, all of which may present differently between patients. WLE is not specific for demarcating tumor margins, which is critical for facilitating the complete removal of malignant tissues that can seed future recurrence of GI cancer. Therefore, the development of advanced imaging technologies, such as those which implement fluorescence imaging, could greatly improve clinical practice by providing tumor-specific contrast with high sensitivity. The vast majority of endoscopes do not feature this imaging modality and are therefore limited to broadband imaging. However, clinical gastroscopes are designed to support the addition of modular accessories.

Reusable clinical gastroscopes contain open channels for the introduction of accessory devices that supplement white light imaging with additional functions, such as biopsy or alternative imaging modalities. The 2.8-mm diameter channel of diagnostic gastroscopes has traditionally posed challenges for introducing imaging devices, which often exceed this diameter. However, the miniaturization of chip-on-tip imaging systems has simplified the development of endoscopes of a compatible size. The clinical value of these miniature, accessory-port imaging instruments is multifold: reductions in outer diameter have enabled endoscopes to traverse narrow anatomical regions that were previously inaccessible, and when used in conjunction with standard reusable gastroscopes, single-use accessory-port endoscopes can be used to supplement the high-resolution gastroscope images with other imaging modalities, including fluorescence. Although this work reports a miniature endoscope designed to operate in conjunction with a clinical system, some design iterations capitalize on a reduction in system scale to image narrow and tortuous anatomical lumens.

On the forefront of advanced miniaturized endoscopy, sub-millimeter scanning fiber endoscopes pave the way for detecting and imaging cancer in regions of the human anatomy that were previously inaccessible via endoscope.[9,10] Some miniaturized systems have now provided access to millimeter-sized lumens for collecting data using autofluorescence, reflectance, and optical coherence tomography modalities.[11] While fiber endoscopes provide powerful imaging capabilities, optical fibers are both expensive and prone to damage from crushing and excess bending, which can result in a reduction in image quality. As a result, chip-on-tip endoscopy as an alternative to fiber endoscopy has gained traction, with some camera module footprints as small as 0.55 mm x 0.55 mm.[12] Because they present affordable and accessible options for flexible, single-use endoscopes and imaging tools, demand for these small sensors is rising. Flexibility and higher resolution, delivered in a compact size, fuel advancement in miniature chip-on-tip endoscopes over existing fiber-based systems for white light and fluorescence modalities.[13,14] While chip-on-tip endoscopes have seen growth, there remains a significant opportunity for improved imaging modalities to increase the sensitivity and specificity of GI cancer diagnosis. Multimodal imaging in chip-on-tip endoscopic screenings for GI cancers may improve contrast between cancerous and noncancerous tissues. Ultimately, a multispectral endoscope, capable

of imaging spectral response in a variety of wavelengths corresponding to unique fluorophores, may serve as a powerful tools for imaging multiplexed fluorophores, each highlighting unique structures or compounds in diagnostic and surgical procedures. In addition to enabling users to detect multiple fluorophores in the same tissue sample, a multispectral endoscope also serves a standalone tool applicable for visualizing a variety of fluorophores without requiring unique hardware for each.

In this brief research report, we present the design, fabrication, and preliminary pre-clinical testing of a miniature multispectral fluorescence endoscope with biopsy capabilities. The device is designed for compatibility with a commercial gastroscope to enable high performance fluorescence imaging of up to four fluorophores. We perform technical characterization of the device and demonstrate ability to measure labeled tissue fluorescence, as well as preliminary results showing sufficient sensitivity to measure autofluorescence. Through the creation of specialized multispectral microendoscope systems designed to detect multiple key fluorescence wavelength bands and collect biopsy material, we advance toward the improved visualization of cancer with enhanced contrast and margin visibility.

Methods

Design & Fabrication

A miniature, biopsy-enabled, chip-on-tip imaging assembly was created to detect fluorescent emissions in four unique wavelength bands without the requisite of changing front-end optics between varying wavelengths. The probe was designed to detect emissions from several fluorophores common in research and clinical settings, including Cy2, Alexa Fluor 488, tdTomato, and Cy5. The design specifications are listed in **Table 1**. Mechanical specifications of size constrained the endoscope to fitting within the working channel of a commercial articulating gastroscope.

Table 1. Specifications of Miniature Multispectral Fluorescence Imaging System

Property	Specification	Purpose
Max. Outer Diameter	≤2.8mm	Enable fit within working channel of commercial gastroscopes (Olympus GIF-HQ190 or Pentax EG-2990i)
Biopsy	Needle or Bite	Preserve tissue architecture for histological analysis
Modalities included	Reflectance, fluorescence	Facilitate navigation and fluorophore detection
Field of View	≥90 degrees	Ensure complete visibility of surrounding lumen walls
Pixel Resolution	>250px x 250px	Enable visualization of tissue morphology for lesion detection

Excitation Wavelengths	405, 488, 561, 640nm	Target up to four common biological fluorophores
Working Distance	5-50mm	Enable visualization along lumen and enable detection of masses
Imaging Mode	Video, photo	Enable real-time detection and data recording
Maximum Rigid Tip Length	10 mm	Enable commercial gastroscope articulation.
Illumination Type	Narrowband via fiber optic	Reduce cost and prevent laser damage
Excitation Wavelength Ranges	405 ± 10nm	Excitation of Coumarin
	488 ± 10nm	Excitation of Cy2, GFP, AF488
	561 ± 10nm	Excitation of tdTomato, DsRed2-C1
	640 ± 10nm	Excitation of Cy5, AF633
Detection Wavelength Ranges	432-456nm	Detection of fluorescence emission for Coumarin
	519-529nm	Detection of fluorescence emission for Cy2, GFP, AF488
	595-605.5nm	Detection of fluorescence emission for tdTomato, DsRed2-C1
	680.5-735nm	Detection of fluorescence emission for Cy5, AF633

Illumination Assembly

The onboard illumination assembly was designed to operate in four distinct wavelength bands to target the absorption peaks from fluorescent compositions with peak excitation wavelengths of 405, 488, 561, and 640 nm (**Figure 1, A**). To provide illumination at each excitation wavelength, four fiber-coupled LED light sources (M405FP1, M490F3, MINTF4, M625F2; Thorlabs, Newton, NJ) were connected via a 400 µm core 1-to-4 fanout fiber bundle (BF44LS01; Thorlabs) to an aspheric condensing lens (ACL2520U-A; Thorlabs). To prevent light leakage into detection bands, each LED was filtered with a corresponding unique 20 nm bandpass filter (FB405-10, FL488-10, FB560-10, FB640-10; Thorlabs) with full-width half-max wavelengths corresponding to the peak absorption wavelengths of a subset of fluorescent probes.

These bandpass filters were mounted in a filter wheel (Thorlabs FW2A) and focused with a second aspheric condensing lens (Thorlabs ACL2520U-A) onto a 1x2 multimode fiber optic coupler (Thorlabs TH400R5F1B), which pairs with two multimode fibers (Thorlabs M136L03) which run through the length of the imaging probe shaft and exit at the distal tip of the device.

Imaging Assembly

A miniature, monochromatic camera, Osiris M (OptaSensor GmbH, Nürnberg, Germany), was selected to perform image acquisition. The 1mm x 1mm x 2mm unit captures images sized at 320 px x 320 px with a pixel size of 2.4 µm.[15] To interface with a computer, signal from the Osiris M is first routed through an external image processing system. To remove eliminate signal from illumination sources, a 1.5 mm x 1.5 mm multiband interference filter (Iridian, Ottawa, ON, Canada) was custom designed to meet the specifications in **Table 1** and fabricated via thin film deposition, impeding the transmission of excitatory illumination wavelengths while simultaneously permitting transmission of desired fluorescence emission wavelengths.

Biopsy Assembly

In the histological characterization of tissues in the luminal GI tract, it is necessary to collect bulk tissue biopsies with forceps (as opposed to needle aspiration) to preserve tissue architecture, a critical feature in histopathological sample analysis. To maintain a miniature footprint, 3 Fr Piranha® biopsy forceps (Boston Scientific M0065051600, Marlborough, MA) were incorporated through a backloading channel and were both introduced and secured using a Hemostasis Valve Y connector (Qosina 97380, Ronkonkoma, NY), featuring a Tuohy Borst adapter with rotating male luer lock and an angled female luer injection side port.

Operator Interface & Device Assembly

To secure components of the imaging system, a cylindrical housing of 2.7 mm in diameter by 10 mm in length with four through-holes was designed in SolidWorks (Dassault Systèmes, Vélizy-Villacoublay, France) and fabricated with stereolithography 3D printing (Elegoo US-SO-3D-110, Shenzhen, Guangdong, China). The terminal ends of the optical fibers were mounted in the lateral through-holes of the cylinder, and Osiris M camera module was positioned in the central through-hole of the printed cylinder such that the multiband filter could then be placed directly in contact with the front of the camera lens, facing outward from the distal tip. The housing was designed so that the fiber channels possessed a subtle curvature to direct the two output beams into a single overlapping illumination region, aligned with the imaging field of view. The biopsy forceps were mounted through the chamber located below the camera module. These components were housed in a stainless-steel shell measuring 3 mm x 14 mm (Microgroup, Medway, Massachusetts). The output illumination fibers were installed through lateral through holes on either side of the camera.

This housing was then inserted into a stylus-like SLA 3D-printed shell composed of rigid resin (Elegoo US-EL-3D-052), which terminates with a flexible, SLA 3D-printed strain relief (RESIONE F69-500g, Dongguan, Guangdong, China) to protect the exiting illumination fibers and cables. This rigid outer shell was designed to be bot durable and larger in diameter to simplify handling during preclinical rodent testing. Clinical presentations of this imaging system are designed such that the length of the endoscope is flexible, with the exception of the final 7mm of the distal tip. All components were secured with a polyvinyl alcohol adhesive generated from DI water and powdered polyvinyl alcohol powder (Sigma-Aldrich 363146-25G, St. Louis, MO).

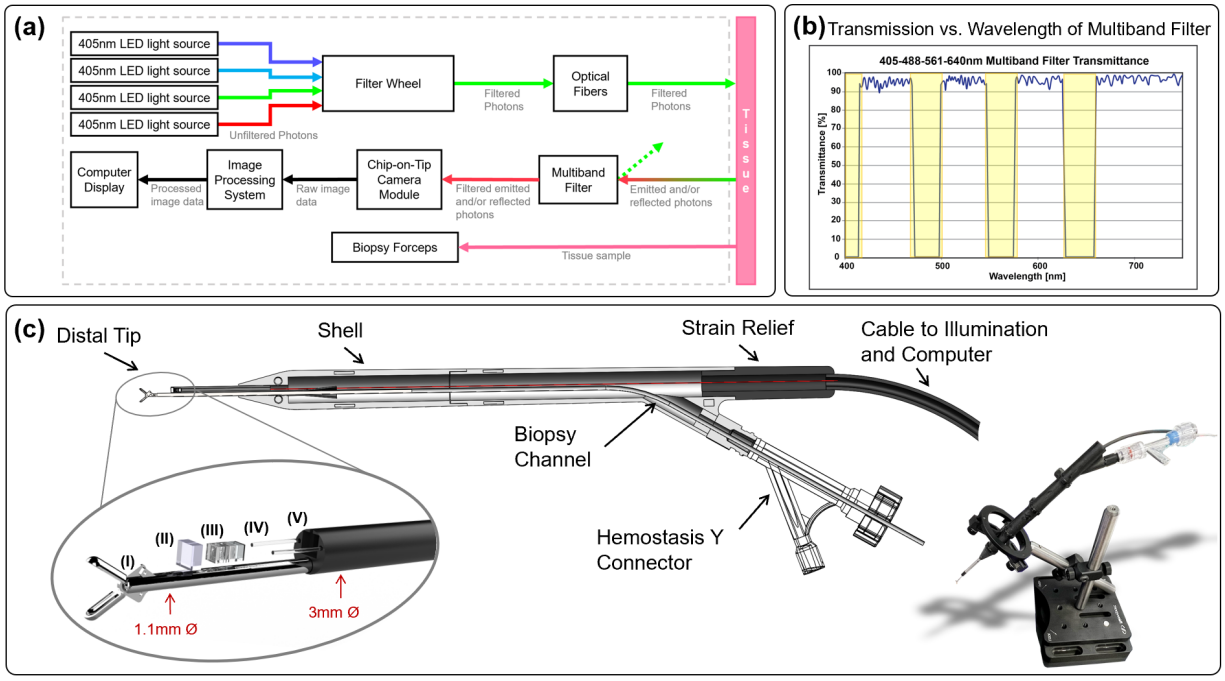

Figure 1. (a) Transmittance of broadband light through custom multiband filter. Highlighted regions indicate wavelengths employed for sample excitation. (b) Block diagram of miniature multiband fluorescence imaging system. (c) Component map of handheld probe. In the magnified image, (I) denotes a pair of Piranha® biopsy forceps. (II) denotes the multiband filter. (III) denotes the miniature chip-on-tip camera module. (IV) indicates the air of optical fibers for illumination. (V) indicates the distal housing.

Device Operation

Image capture, video capture, and camera settings control are controlled by means of a custom digital interface (OptaSensor, IPS Viewer v01_07) through USB3.0 connection. Onboard illumination is operated using **UPLED** software (Thorlabs) to adjust source brightness through current titration. For preliminary evaluation, manipulation of the device was performed by translation of the device body, ensuring the distal tip is pointing toward the target of interest, confirmed by visually inspecting the output image to ensure that the field of view is centered and the image is in focus. A custom mount with a stand was designed to secure the device to allow for stationary imaging **(Figure 1, c)**. Fluorescence imaging may be toggled by switching between illumination sources. Reflectance imaging can be achieved using broadband illumination or narrow band illumination in wavelengths within the transmission ranges accepted by the distal tip multiband filter.

To collect a biopsy, two hands are required in instances in which the device is not mounted and stationary. In this configuration, the biopsy forceps are run through the Touhy Borst at the proximal end of the Qosina Y connector. Next, the user tightens the extended forceps such that they are both in contact with tissue and sufficiently visible to the camera. The imaging device is handled by the user's dominant hand, and the biopsy mechanism is activated by the user's non-dominant hand. In instances in which the imaging system is mounted and stationary, this process may be performed with one hand. Collected tissue samples may then be retrieved by loosening the Touhy Borst and retracting the closed biopsy forceps from the forceps subchannel.

Characterization

Slanted-Edge Modulation Transfer Function Characterization

To assess resolution, the modulation transfer function (MTF) was measured in a configuration that simulated contrast conditions during normal use: fluorescent illumination against a non-fluorescent margin, and the slanted-edge MTF analytical technique was employed. This technique is derived from the edge-gradient analysis algorithm, but distinctly operates with an image input of a sharply contrasting linear interface aligned such that it does not fall precisely along a row or column of individual sensors a camera's sensor array.[16] To perform the analysis, test images were captured of the interface of a slightly tilted, sharpened blade against a fluorescent standard slide (CHROMA, Bellows Falls, VT), back-illuminated with the 405 nm LED light source. The ImageJ plugin *SE_MTF* was used to select a region crossing the slanted edge interface of the sharpened blade and fluorescently illuminated background slide to subsequently yield the modulation transfer function of the system in cycles/pixel.[17]

Geometric Distortion

Geometric distortion is a measure of how the magnification of an optical system varies across the image. This is a common effect seen in imaging systems with large fields of view such as in endoscopic imaging. Correction measures can be implemented during postprocessing, provided that the degree and type of distortion are well-characterized. Distortion of the system was measured using a grid target (ThorLabs, R2L2S3P4). To calculate distortion, the target grid was placed such that the pattern filled the field of view of the camera. Images were captured and imported into ImageJ where the distance from the image center of diagonal grid points was measured and the deviation from linearity was recorded.

Fluorescence Sensitivity

To measure fluorescence sensitivity, serial dilutions were performed from a stock solution of a known concentration of Fluorescein, and the resulting dilutions were transferred to standard 1 cm x 1 cm spectrometry cuvettes. The cuvettes were illuminated with the device using the 488 nm LED and images were collected for each concentration. Images were analyzed by calculating the mean image brightness for each concentration in a stationary region of interest to detect the illumination level at which the sensor is sensitive to the presence of fluorescent emission.

Preclinical Studies

Biopsy Quality Verification

Tissue samples were collected from the lumens of excised murine duodenums using Piranha® biopsy forceps tracked through the fluorescence probe subchannel. To confirm that tissue biopsied with the Piranha biopsy forceps maintains sufficient cell architecture for histopathology, tests to assess biopsy quality were performed. Quality was determined by the assessment of the usability of stained samples for identification of cell types, GI tissue architecture, and tissue orientation.

To perform this assessment, the Piranha biopsy forceps were used to collect tissue samples from the lumen of a freshly necropsied murine duodenum. Samples were fixed in 4% paraformaldehyde, prepared in d-sucrose, and then embedded in O.C.T. (optimal cutting temperature) compound. Tissue was cryosectioned and stained according to a standard hematoxylin and eosin (H&E) protocol. Following staining, tissue quality assessment was performed by the identification of crypts and villi, fragile but crucial landmark structure within duodenal tissue, via light microscopy.

Ex vivo Fluorescence Detection in Gastrin CreERT2; ZsGreen Models

For preliminary validation of *ex vivo* fluorescence performance, a study was performed with transgenic mouse model *Gastrin CreERT2; ZsGreen*. In a cohort of eight mice, a ZsGreen fluorescent reporter was conditionally expressed in G cells using a Gastrin-driven Tamoxifen-inducible Cre recombinase (Gastrin-CreERT2). Beginning at 6-weeks of age, mice were administered 0.1 ml of 20 mg/ml of Tamoxifen five times per month for three months to induce ZsGreen expression in G cells. Following necropsy, the stomach and proximal duodenum were removed, opened to expose the lumen, and flushed with ice-cold phosphate buffered saline prior to imaging.

The imaging system was configured with the distal tip 2-3 cm above samples of *ex vivo* murine stomach and duodenal tissue. An external light source (Lambda LS, Sutter Instruments, Novato CA) was used to illuminate sections of mouse GI tissue in a petri dish, and images were captured with both broadband unfiltered light and 488 nm (FB560-10, Thorlabs) filtered illumination for excitation of ZsGreen. Images were captured and fluorescence detection data were digitally enhanced and overlayed upon the broadband light images to create a composite highlighting the signal-producing regions of the GI tract.

Examination of Tissue Autofluorescence Capabilities

To assess if the device is sufficiently sensitive to collect autofluorescence, a portion of the GI tract from forestomach to duodenum, brain, lung, and pancreatic tissues was excised from healthy, unlabeled wild type mice via necropsy. These sections were briefly placed on ice in a petri dish with PBS and fluorescent images were collected with both the multiband fluorescence imaging probe and a previously-reported Multispectral Fluorescence Imaging System (MSFI) at four distinct wavelengths: 400nm, 490nm, 543nm, and 560nm, wherein 560nm serves as reflectance imaging wavelength and 400nm, 490nm, and 560nm serve as fluorescence emission imaging wavelengths [18].

Results

Device Construction and Characterization

Resolution/MTF

Analysis of the slanted-edge MTF method yielded the line spread function and the MTF. The MTF_{50} of the system is 0.2 cycles/pixel. The cutoff frequency for this system was determined to be 0.35 cycles/pixel. Due to the inverse relationship between cutoff frequency and resolution, the resolution of the system can be estimated as approximately 6.72µm.

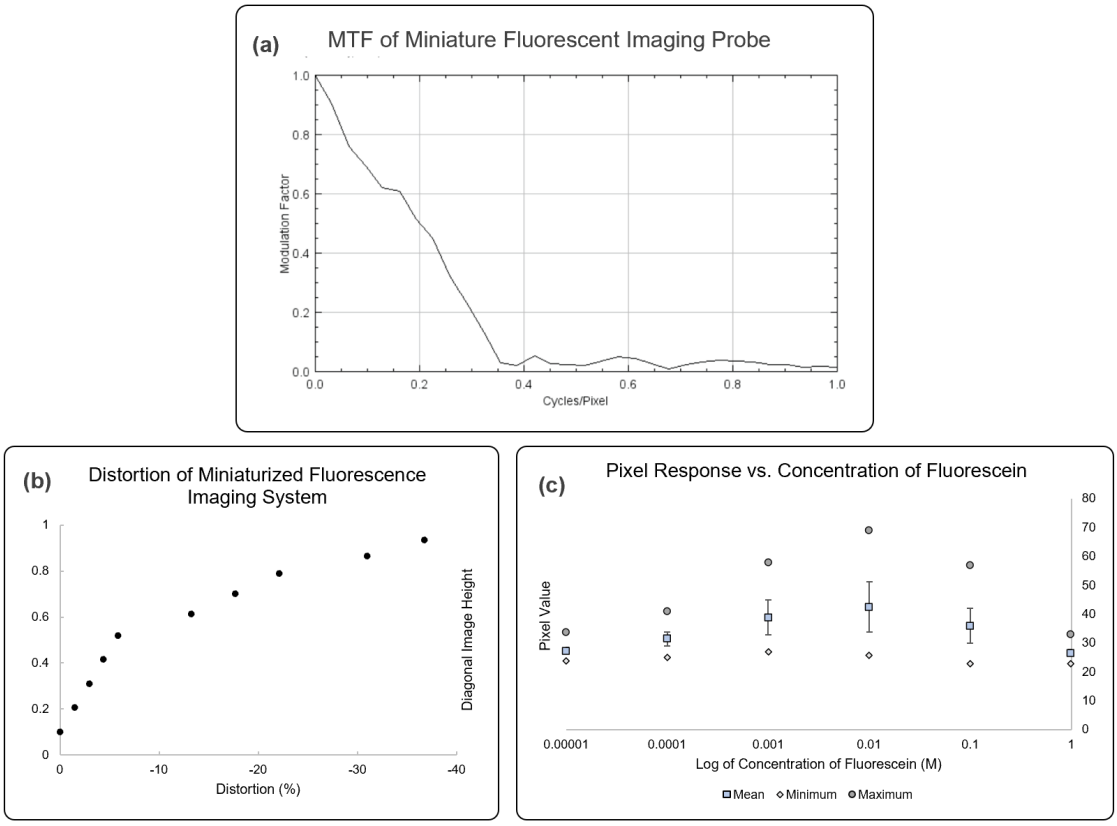

Figure 2. (a) MTF of miniaturized multiband fluorescence imaging system. (b) Distortion of miniaturized multiband fluorescence imaging system. (c) Pixel response versus fluorescein concentration for miniaturized multiband fluorescence imaging system.

At the corners of the image, the maximum distortion was measured as -36% deviation from predicted values.

Detected signal increased with increasing concentration until signal was maximized at 0.01M of fluorescein, with this concentration displaying the highest pixel overall pixel value and highest average. It was confirmed that, at high concentrations, the fluorophores exhibited diminished levels of fluorescence as a result of self-quenching, the process by which intermolecular reactions between identical fluorophores inhibits fluorescent emission.[19] When measured using on-board illumination set to a maximum power output of 1.21µw at 561 +/- 10 nm, results from this test support sensitivity to evenly dispersed fluorescein concentrations as low as 10^{-5} M in a standard 1 cm x 1 cm cuvette.

Preclinical Testing

The resulting H&E slides were imaged under a light microscope, and analysis of bright-field images confirmed that duodenal biopsies collected with the Piranha biopsy forceps preserved tissue architecture for histological observations. Crypts, villi, and other structural features were well-preserved, allowing for the clear discernment of tissue orientation, invaluable for assessing biopsied tumor tissue.

Images captured of *ex vivo* murine GI tissue indicate the presence of fluorescence in the antrum of the stomach, the region in which gastrin-secreting G cells are located. The expression of ZsGreen was additionally confirmed by fluorescence microscopy of cryosectioned antral tissue.

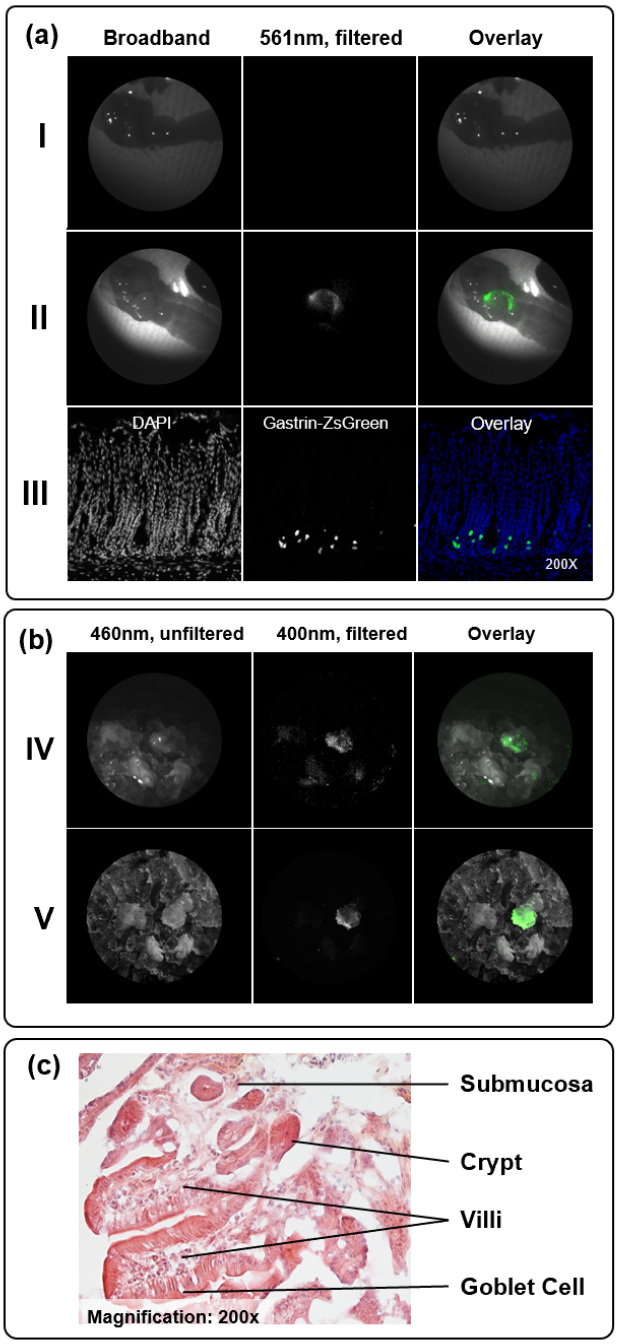

Figure 3. (a) Rows (I) and (II) reflect images captured with the miniature multiband fluorescence imaging system; wherein row (I) depicts antrum specimens from control mice and row (II) depict antrum specimens from transgenic Gastrin CreERT2; ZsGreen mice. Row (III) contains fluorescence microscopy images captured of the transgenic antrum specimens from the previous row at

200x magnification. In rows (II) and (III), fluorescence is indicated in overlay images as bright green. Photos have been brightened and have had the contrast increased for visibility. **(b)** Row (IV) contains images of brain, liver, lung, and GI tissue in a petri dish captured by the miniature multiband fluorescence imaging system collected with 460nm illumination and 400nm (filtered) illumination in addition to an overlay image in which fluorescent detection is depicted as green. Row (V) contains images collected by the high-resolution MSFI system at both 460nm and 400nm (filtered) and contains an overlay image to combine fluorescent emissions (green) with contextual unfiltered imaging. Photos have been brightened and have had the contrast increased for visibility. **(c)** An H&E biopsy sample of murine duodenum, 200x magnification, collected with Piranha® biopsy forceps demonstrates extraction and preservation of crypts and villi for histopathology.

Examination of Tissue Autofluorescence Capabilities

Detectable levels of autofluorescence were recorded by the miniature multiband fluorescence imaging system in the forestomaches of unlabeled mice. This finding was corroborated by high resolution images captured by the external MSFI system. Fluorescent artefacts were noted in images captured with both systems. Tissues were further analyzed under fluorescence microscopy to eliminate the possibility of contamination with exogenous fluorescent moieties, with no evidence of contamination found.

Discussion

Device Design & Configuration

At less than 3 mm in diameter, the component that spaces and houses each piece was particularly challenging to create without resorting to costly and time-consuming methods like wire EDM. The simplest alternative that supports creating designs for swift iteration is 3D printing. Yet, most commercial 3D printers are do not possess sufficient resolution to reliably print pieces with through-holes less than one third of a millimeter in diameter. On the other hand, printers like those created by Nanoscribe, are specially design for prints much less than 3mm in diameter. The resulting gap in manufacturing methods threatened to redirect the course of design for this system until a solution was found through a highly versatile and accessible consumer SLA 3D printer.

Characterization

The low system resolution can be attributed to several limitations imposed by both the physical system and test method which, were not representative of diffraction-limited conditions. First, the camera module, which pushes the limits of present manufacturing capabilities, is generated through the adhesion of a series of optical components that likely result in a degree of aberration due to coma and spherical aberration. As a consequence of performing this MTF analysis in a setting to mimic general use, parameters like low contrast and a wide range of illumination wavelengths serve to reduce contrast and induce chromatic aberration, further reducing measured valued of resolution. Resulting from the nature of the fluorescence emission of the backlit slide, the imaged interface does not exhibit a sharp, well-contrasted interface. Since the illumination was configured to simulate typical application of the imaging system, the contrast between the blade edge and fluorescing slide is less than that of the blade and a bright white background. The MTF values gained from this analysis serve as conservative estimates of device functionality in dimly emissive environments. The resolution measurements support the capabilities of the system while also highlighting room for improvement. As miniaturized sensors continue to advance, we can anticipate higher resolution in the same or smaller sensor footprints with improvements to performance in low-light settings.

In instances of geometric distortion, images captured do not reflect the reality of the proportions of objects imaged as a result of a relationship between magnification and height within the

optics of the camera module. In this wide-angle (fisheye?) camera module, barrel distortion is evident, indicating that objects captured near to the center of the field of view occupy a larger proportion of the overall frame than objects imaged at the periphery. Once quantified, geometric can be corrected during image post-processing.

Although the imaging system successfully detected highly dilute levels of fluorescein, few resources exist to quantify how sensitive a system must be to adequately perform in bioscience fluorescence applications, thus additional verification in biological models will be necessary. Although quantum efficiency is inherently low with the Osiris M, at about 20% for much of the visible spectrum, it can also be tied to the level of illumination achieved by this system. Because it employs four unique fiber-coupled LED sources, each with specific amperages, the resulting illumination varies drastically with wavelength. At conception, this device was designed with work with a single, powerful xenon source. However, LEDs have proven more cost-effective and safer than alternatives like lasers. Likewise, there is a lower probability of photo-bleaching a sample with the reduced levels of emitted light from LEDs. Despite high costs and safety hazards, increasing light output may also serve as an effective manner to increase perceived system sensitivity without adjustments to camera modules, should advancements in miniature camera sensitivity be currently unattainable.

Preclinical Testing

Results from biopsy collection confirmed that miniature bite biopsy performed with 3 Fr Piranha forceps yields meaningful structural information that could be used to identify hyperplastic and dysplastic tissues in regions identified as potentially cancerous.

Images captured of fluorescent ZsGreen signal localized to the antrum support that the miniature multiband fluorescence imaging system is capable of accurately detecting concentrations of fluorescent moieties within labeled tissue. From fluorescent microscopy images, it is evident that only a small proportion of cells, presumably g-cells, were producing the fluorescent protein, although detection was both clear and concentrated, suggesting that the device has high sensitivity.

Images captured by both the high-resolution MSFI and the miniature multiband fluorescence imaging system display marked similarity in tissue autofluorescence pattern. However, images captured by the miniature system are more than 200x smaller, resulting in a significant loss of detail, and the overall bit depth of the system is much lower. Between the two systems, images from the miniature imaging device possessed more visual artefacts with a lower signal-to-noise ratio, although the miniature system also performed with a much short exposure window, at just fractions of a second. With additional adjustments for gain and thresholding, fluorescent regions could be made more discrete. Despite the high optical density, light leakage around the edges of the multiband filter appear to occasionally interfere with the signal quality. Some artefacts are likely to be the result of the tissue-preserving medium. The tissues were imaged in an ice bath to preserve tissue quality for histopathology; consequently, the irregular ice particles refracted emitted fluorescence from tissue such that the ice itself appeared to be generating signal.

Conclusion

We present the design and characterization of a miniature, handheld, chip-on-tip fluorescence imaging probe with a front-end multiband filter for the imaging of multiplexed fluorophores to aid in the localization of labeled cancerous lesions. Preliminary testing of the imaging system produced viable

images of real-time fluorescence while systematically preventing excitatory light from reaching the detector. Demonstrations of the miniature fluorescence imaging system indicate successful fabrication for detection of multiple fluorescent species and collection of biopsy specimens.

References

[1] Y. Aisu, D. Yasukawa, Y. Kimura, and T. Hori, "Laparoscopic and endoscopic cooperative surgery for gastric tumors: Perspective for actual practice and oncological benefits," *World J. Gastrointest. Oncol.* **10**, 381 (Baishideng Publishing Group Inc, 2018).

[2] M. Gutowski, B. Framery, M. C. Boonstra, V. Garambois, F. Quenet, K. Dumas, F. Scherninski, F. Cailler, A. L. Vahrmeijer, et al., "SGM-101: An innovative near-infrared dye-antibody conjugate that targets CEA for fluorescence-guided surgery," *Surg. Oncol.* **26**, 153–162 (Elsevier, 2017).

[3] R. P. J. Meijer, K. S. de Valk, M. M. Deken, L. S. F. Boogerd, C. E. S. Hoogstins, S. S. Bhairosingh, R. J. Swijnenburg, B. A. Bonsing, B. Framery, et al., "Intraoperative detection of colorectal and pancreatic liver metastases using SGM-101, a fluorescent antibody targeting CEA," *Eur. J. Surg. Oncol.* **47**, 667–673 (W.B. Saunders, 2021).

[4] "Phase I of SGM-101 in Patients With Cancer of the Colon, Rectum or Pancreas - Full Text View - ClinicalTrials.gov," <https://www.clinicaltrials.gov/ct2/show/NCT02973672?term=sgm-101&draw=2&rank=1> (22 April 2022).

[5] de Valk, al P. Ruben J Meijer, K. S. de Valk, B. Framery, M. Gutowski, A. Pèlegrin, F. Cailler, D. E. Hilling, and A. L. Vahrmeijer, "The clinical translation of a near-infrared fluorophore for fluorescence guided surgery: SGM-101 from the lab to a phase III trial," *https://doi.org/10.1117/12.2555598* **11222**, 73–78 (SPIE, 2020).

[6] E. Figueras, A. Martins, A. Borbély, V. Le Joncour, P. Cordella, R. Perego, D. Modena, P. Pagani, S. Esposito, et al., "Octreotide Conjugates for Tumor Targeting and Imaging," *Pharm. 2019, Vol. 11, Page 220* **11**, 220 (Multidisciplinary Digital Publishing Institute, 2019).

[7] R. Singh, V. Owen, A. Shonde, P. Kaye, C. Hawkey, and K. Ragunath, "White light endoscopy, narrow band imaging and chromoendoscopy with magnification in diagnosing colorectal neoplasia," *World J. Gastrointest. Endosc.* **1**, 45 (Baishideng Publishing Group Inc, 2009).

[8] Y.-H. Song, L.-D. Xu, M.-X. Xing, K.-K. Li, X.-G. Xiao, Y. Zhang, L. Li, Y.-J. Xiao, Y.-L. Qu, et al., "Comparison of white-light endoscopy, optical-enhanced and acetic-acid magnifying endoscopy for detecting gastric intestinal metaplasia: A randomized trial.," *World J. Clin. cases* **9**, 3895–3907 (Baishideng Publishing Group Inc., 2021).

[9] J. J. McGoran, M. E. McAlindon, P. G. Iyer, E. J. Seibel, R. Haidry, L. B. Lovat, and S. S. Sami, "Miniature gastrointestinal endoscopy: Now and the future," in *World J. Gastroenterol.* **25** (Baishideng Publishing Group Inc, 2019).

[10] S. J. Miller, C. M. Lee, B. P. Joshi, A. Gaustad, E. J. Seibel, and T. D.-S. Wang, "Targeted detection of murine colonic dysplasia in vivo with flexible multispectral scanning fiber endoscopy," *J. Biomed. Opt.* **17**, 021103 (SPIE, 2012).

[11] K. C. Kiekens, G. Romano, | Dominique Galvez, R. Cordova, | John Heusinkveld, | Kenneth Hatch,

W. Drake, Z. Kmeid, and J. K. Barton, “Reengineering a falloposcope imaging system for clinical use” (2020).

[12] OMNIVISION, “OH0TA10-A04A,” <https://www.ovt.com/products/oh0ta10-a04a/> (25 April 2022).

[13] M. R. Gaab, “Instrumentation: Endoscopes and Equipment,” *World Neurosurg.* **79**, S14.e11-S14.e21 (Elsevier, 2013).

[14] G. Matz, B. Messerschmidt, W. Göbel, S. Filser, C. S. Betz, M. Kirsch, O. Uckermann, M. Kunze, S. Flämig, et al., “Chip-on-the-tip compact flexible endoscopic epifluorescence video-microscope for in-vivo imaging in medicine and biomedical research,” *Biomed. Opt. Express* **8**, 3329 (Optical Society of America, 2017).

[15] OptaSensor GmbH, “Osiris M Module Product brief.”

[16] P. D. Burns, “Slanted-Edge MTF for Digital Camera and Scanner Analysis,” in *Soc. Imaging Sci. Technol. Image Process. Image Qual. Image Capture, Syst. Conf.*, (2000).

[17] C. Mitja, J. Escofet, A. Tacho, and R. Revuelta, “Slanted Edge MTF - Image J,” 2011, <https://imagej.nih.gov/ij/plugins/se-mtf/index.html> (7 January 2022).

[18] N. Lima and T. W. Sawyer, “Design and validation of a multispectral fluorescence imaging system for characterizing whole organ tissue fluorescence and reflectance properties,” in *Multiscale Imaging Spectrosc. III*, K. C. Maitland, D. M. Roblyer, and P. J. Campagnola, Eds., (SPIE, 2022).

[19] X. Zhuang, T. Ha, H. D. Kim, T. Centner, S. Labeit, and S. Chu, “Fluorescence quenching: A tool for single-molecule protein-folding study,” *Proc. Natl. Acad. Sci. U. S. A.* **97**, 14241–14244 (2000).